Optimisation and application of an analytical approach for the characterisation of TiO2 nanoparticles in food additives and pharmaceuticals by single particle inductively coupled plasma-mass spectrometry

Lucas Givelet, Delphine Truffier-Boutry, Laurent Noël, Jean-François Damlencourt, Petru Jitaru, Thierry Guérin

Optimisation and application of an analytical approach for the characterisation of TiO_2 nanoparticles in food additives and pharmaceuticals by single particle inductively coupled plasma-mass spectrometry

Lucas Givelet[a,b], Delphine Truffier-Boutry[b], Laurent Noël[c], Jean-François Damlencourt[b], Petru Jitaru[a], Thierry Guérin[a]

[a] Anses, Laboratory for Food Safety, F-94701 Maisons-Alfort, France

[b] Univ. Grenoble Alpes, CEA, LITEN, F-38000 Grenoble, France

[c] The French Directorate General for Food, Ministry of Agriculture, Agro-16 Food and Forestry, F-75015 Paris, France

Corresponding author: thierry.guerin@anses.fr; ORCID ID 0000-0003-4060-6616

Anses, Laboratory for Food Safety

14, rue Pierre et Marie Curie

F-94701 Maisons-Alfort, France

Abstract:

This study was designed to optimise an analytical method for characterising TiO_2 nanoparticles (NPs) in food additives and pharmaceuticals by inductively coupled plasma-mass spectrometry in single particle mode (spICP-MS). Several parameters, including transport efficiency (TE), were assessed and optimised using the NM-100 reference material. We found that self-aspiration for sample intake and use of the concentration-based method for TE was optimal for characterising TiO_2 NPs. No spectral interference was observed with either ^{49}Ti or ^{48}Ti isotopes. The optimised Excel spreadsheet developed for this study not only provided additional parameters but gave results closer to the NM-100 reference value than the ICP-MS software. The method was then applied to the analysis of a selection of food samples and pharmaceuticals. The average diameter of TiO_2 particles ranged from 86 to 179 nm in the food samples and from 131 to 197 nm in the pharmaceuticals, while the nanoparticular fraction was between 19 and 68% in food, and between 13 and 45% in pharmaceuticals.

Keywords: spICP-MS, TiO_2 nanoparticle, E171, threshold, data processing, food & pharmaceutical

1. Introduction

Due to their specific properties, nanomaterials have been employed for two to three decades in many fields, such as construction [1,2], medicine [3,4], cosmetics [5,6] and the food industry [7,8]. Among all the manufactured nanomaterials available, this study focused on those containing TiO_2 nanoparticles (named "E171" by the European Parliament [9]; E171 is used only for food-grade TiO_2 and is only valid for Europe), which have been widely used in the food industry as an ingredient in various food products. A regulation stating that "all ingredients present in the form of engineered nanomaterials shall be clearly indicated in the list of ingredients" was published in 2011 [10]. The names of such ingredients should be followed by the word 'nano' in brackets. However, the identification and traceability of nanomaterials in foodstuffs remain limited even today due to the coexistence of non-harmonised definitions [11]. It is worth noting that TiO_2 exists in three different crystallographic forms: *anatase*, *rutile* and *brookite*. TiO_2 in the form of *anatase* is the most used in the food industry [12–14]. This additive was not initially considered as a nanomaterial because most of the TiO_2 it contains is found predominantly at micrometric scale. However, recent studies showed that E171 contains a non-negligible fraction (≅10-50%) of TiO_2 in the form of nanoparticles (NPs) [8,12,15–17], which correspond to particles < 100 nm [10]. This is of particular concern because TiO_2 is classified by the International Agency for Research on Cancer (IARC) as a possible human carcinogen when inhaled [18]. The European Food Safety Authority (EFSA) does not question the use of TiO_2 in food [19–21], although several studies have reported that TiO_2 NPs may increase the risk of accelerating existing cancer processes [22–24]. Nevertheless, developing accurate analytical methods with which to characterise TiO_2 NPs in foodstuffs is still very challenging. Imaging-based techniques such as scanning electron microscopy (SEM) and transmission electron microscopy (TEM) are the most widely-used nowadays [15,17,25–27], followed by techniques based on light scattering such as dynamic light scattering (DLS) and multi-angle light scattering (MALS). Separation techniques such as field flow fractionation (FFF), centrifugal particle sedimentation (CPS) are also used to characterise NPs [28–30]. In recent years, inductively coupled plasma-mass spectrometry in single particle mode (spICP-MS) has been increasingly used for NP characterisation. This method was first reported in the 2000s [31–34], though its theoretical aspects have been refined more recently [35–37]. Although spICP-MS has the advantage of simultaneously sizing and quantifying metal and metal oxide NPs in various matrices, it requires the accurate optimisation of several experimental parameters. These include transport efficiency (TE) [37–41], dwell time [28,42,43] and the threshold calculation to discriminate NP events from the background [37,44–47]. The data processing related to these parameters also needs to be improved to obtain a more accurate characterisation of NPs by spICP-MS.

This study thus focuses on the optimisation of an spICP-MS method for the qualitative and quantitative characterisation of TiO_2 NPs in the E171 food additive. A reference material (NM-100) containing TiO_2 NPs previously characterised within the framework of the Nanogenotox project [48] and by the Joint Research Centre (JRC) [49] was used for method optimisation. The dwell time, the threshold for counting NPs, the monitoring of isotopes and the TE calculation method were all optimised to achieve an accurate characterisation of TiO_2 NPs. The optimised Excel spreadsheet developed in this study was also compared with the ICP-MS software. The method was then applied to the characterisation of TiO_2 particle size distribution in several foodstuffs and pharmaceuticals.

2. Material and Methods

2.1 Reagents and samples

The NM-100 (*anatase*) reference material (RM) used in this study has a primary TiO_2 particle diameter between 16.4 and 661.6 nm, with an average diameter of 162.4 ± 4.3 nm and a nanoparticular fraction of 27.1% based on the equivalent circle diameter result obtained with transmission electron microscopy (TEM). E171 (powder) was purchased from Fiorio Colori Spa (Gessate, Italy). Ionic gold (1000 µg/L), titanium (1000 µg/L) and calcium (1000 µg/L) standard stock solutions were purchased from Astasol (Prague, Czech Republic). Ammonium sulphate (99.999%), magnesium chloride (≥ 98%) and sodium hydrogen phosphate (> 98%) were purchased from Sigma (Steinheim, Germany). Gold NPs (20, 40, 50, 60, 80 and 100 nm) from BBI Solutions (Cardiff, United Kingdom) were used to calibrate the ICP-MS measurements for TE determination. Nitric (67-69%) and acetic (Normapur, > 99.8%) acids were purchased from Normatom (Leuven, Belgium), Merck (Darmstadt, Germany) and VWR (Leuven, Belgium). The ultrapure water (18.2 mΩ) was produced by a Milli-QTM system from Millipore (Saint-Quentin-en-Yvelines, France). All solutions and dispersions were prepared in polypropylene flasks (Perkin Elmer, Courtaboeuf, France). Eleven food products such as chewing gum, chocolate, frozen desserts or pastries containing TiO_2 NPs were purchased in 2019 from different French supermarkets. A product for which it was claimed that E171 had been removed from its composition was also purchased for confirmation. Four common pharmaceuticals were obtained from a local pharmacy at the same time. More details concerning the samples analysed in this study are presented in the supplementary material (SM Tables A1-A2).

2.2. Instrumentation

A sonication bath (Model 86483, Fisher Bioblock, Rungis, France) was used throughout for the homogenisation of stock NP dispersions before their dilution. An iCapQ ICP-MS from Thermo Scientific (Courtaboeuf, France) was used to characterise NPs in single particle mode. The optimum parameters used for spICP-MS are described in SM Table A3.

2.3. Sample preparation

2.3.1. NM-100

The NM-100 reference material was used to optimise the spICP-MS method. For this purpose, a stock dispersion at 1000 mg/L was prepared in ultra-pure water and stored at 4°C for no more than 1 year. For each analysis, a dispersion at 1.0 µg/L was prepared (n = 3) from the stock one after its homogenisation by sonication for 10 min.

2.3.2. Extraction of NPs from foodstuffs and pharmaceuticals

The extraction protocol used in this study is a simplified version of the procedure reported by Chen et al. (2013) [15]. Briefly, 0.1 - 2.0 g of sample was extracted with ultra-pure water assisted by sonication for 10 min. An aliquot of the obtained dispersion was diluted with nitric acid (0.1% v/v) in order to obtain a concentration of 25,000-100,000 particles/mL (checked by spICP-MS analysis) which gave a signal/noise ratio for all the signals of around 10%, as recommended for a 10 ms dwell time [42,50]. For the frozen desserts and pastries, only a specific part of the sample was taken for analysis; consequently, these data are not representative of the whole food (details are given in SM Tables A1-A2). Finally, the dilution factors could vary between 1500 and 500,000 depending on the samples, thus reducing potential non-spectral interferences e.g. ^{48}Ca or $^{36}Ar\ ^{12}C$ for ^{48}Ti or or $^{37}Cl\ ^{12}C$ for ^{49}Ti [51].

2.4. spICP-MS analysis

2.4.1. Assessment of transport efficiency and system calibration for intensities to diameter conversion

To assess transport efficiency (TE), the spICP-MS system was calibrated using four standard solutions of ionic gold (0, 0.5, 1 and 2 µg/L) prepared in nitric acid (0.1% v/v). A dispersion of gold NPs at 50 nm and about 45,000 particles/mL, previously sonicated at maximum power for 5 min, was further analysed in triplicate. The solvent used to prepare Au NP dispersion and ionic solutions was also used to prepare the TiO_2 NPs dispersions. TE was calculated by size-based and concentration-based methods as reported by [37].

Finally, the flow rate of the sample intake was assessed daily (in duplicate) by weighing the mass of ultrapure water aspirated over a period of at least 5 min. The uptake flow rate was determined from the volume and the uptake time.

To convert the measured intensities into NP diameters, seven standard solutions of ionic titanium (0, 0.25, 0.5, 1, 2, 5 and 10 µg/L) prepared in nitric acid (0.1% v/v) were used for calibration.

2.4.2. Analysis and data processing

Before analysis, the NP dispersions were homogenised by vortex agitation for 5 - 10 s. The samples were then analysed by spICP-MS in standard mode using the high sensitivity option (STDS); the intensity data were recorded using the npQuant module of the Qtegra ISDS software (version 2.8.2944.202) and exported to an Excel spreadsheet (Microsoft®) for further processing. A comparison of the optimised Excel spreadsheet and of the capacity of ICP-MS software is presented hereafter. NPs were considered spherical and with a density of 3.9 $g.cm^{-3}$, which corresponds to the density of the *anatase* structure [52].

3. Results and discussion

3.1. spICP-MS optimisation

The main parameters having an impact on spICP-MS measurements were optimised as presented hereafter. The influence of dwell time on the average diameter and nanoparticular fraction of NM-100 RM was assessed over a range from 0.5 to 100 ms for the analysis of a dispersion of 1 µg/L in ultrapure water with an acquisition time of 3 min (SM Fig. A1). The best results were obtained with a dwell time of 5 and 10 ms, which is consistent with the results reported by Mitrano et al. (2012) [28]. Shorter or longer dwell times underestimated or overestimated the average diameter and the nanoparticular fraction of TiO_2 in NM-100 RM. This is due to the probability of splitting the particles or the acquisition of a signal for more than two particles per dwell time frame [28]. A dwell time of 10 ms was then used throughout the study to minimise the quantity of data and facilitate data processing.

To efficiently distinguish the particle signal from the background noise, a threshold was assessed between 3- to 6-fold the standard deviation (SD) of the raw data obtained on the NM-100 RM (SM Fig. A2), in keeping with the methodology reported by Pace et al. (2011) [37]. Only the 3×SD criterion (SM Fig. A2A) takes into account background noise around 20 - 40 nm; the other size distributions do not reveal any significant difference according to Student's paired t-test (n=3, p=0.05). The 4×SD criterion was chosen to achieve the best size limit of detection (sLOD).

To improve the sLOD, the spICP-MS signal stability obtained either by using peristaltic pumping or the self-aspiration intake system was assessed by analysing several blanks (ultrapure water) at a flow rate of

approximately 0.40 mL/min (SM Fig. A3). Due to the considerably lower background noise, the self-aspiration intake system was chosen for further experiments as previously observed by Venkatesan et al. (2018) [53].

As only a single isotope can be acquired at any one time by spICP-MS, several Ti isotopes were assessed by analysing a solution of ionic titanium (3 µg/L) spiked with a mixture of various interfering elements such as S, Cl, P, C and Ca at different levels, using the (conventional) ICP-MS method and external calibration (and Sc as an internal standard). The isotopes that were subject to the least and most interference respectively were ^{49}Ti and ^{48}Ti (SM Fig. A4). In subsequent experiments, the ^{48}Ti isotope (the most abundant but also subject to the most interference by ^{48}Ca) and ^{49}Ti (the least subject to interference) were used for spICP-MS measurements.

The optimisation of TE is primordial as this parameter is the main factor influencing the accuracy of spICP-MS measurements. Two methods — size-based and concentration-based — are generally used to obtain good accuracy. Contrary to the results observed by Pace et al. (2011) [37], recent studies have reported a significant difference between these approaches [38,40]. Hence, in this study, the TE was optimised carefully by assessing three different procedures, as described below.

The first procedure relied on the analysis of gold NPs of different diameters (20, 40, 50, 60, 80 nm) using the conditions described in section 2.4.2. As can be seen in Fig. 1, the size-based method provides more accurate diameter determination, which is also in agreement with recent studies [39,40].

The second procedure relied on the analysis of NM-100 RM (n=9), whose concentration in terms of TiO_2 NPs is known. The results calculated with the two methods varied by 18% for the diameter and by 34% for the nanoparticular fraction (Fig. 2). This confirms that the method used to assess TE has a significant impact on the accuracy of spICP-MS measurements when characterising TiO_2 NPs. The TE calculated using the concentration-based method provides more accurate diameter and nanoparticular values than the size-based method.

For the third procedure, a sample of E171 that had been previously characterised in terms of average diameter and nanoparticular fraction [12,14] was analysed.

The results in terms of average diameter (Fig. 3a) are in agreement with those obtained by Jovanović et al. (2016) [13] using the TE concentration-based method. Regarding the nanoparticular fraction (Fig. 3b), the closest result to the other studies is also that obtained using the concentration-based method. Like for the analysis of the NM-100 reference material, the differences between diameters measured using the TE assessed with the two methods are significant (up to 50 nm). However, as some of the results reported in Fig. 3a-b were obtained with different analytical techniques such as TEM [8,12], atomic force microscopy or dynamic light scattering [13], it is difficult to conclude on the most accurate values. To conclude, the optimisation of TE by the

concentration-based method was estimated more appropriate for characterising TiO_2 NPs (NM-100 and E171) and was therefore selected to analyse real-life samples.

3.2. Data processing optimisation

The data obtained by spICP-MS can be processed using the npQuant module, which is part of the QTegra platform of the ICP-MS used. The main advantage of the npQuant module is that it allows fast data processing, but it should be stressed that this module has limitations in terms of the parameters available, lacks flexibility and provides no information on data processing protocols. It was therefore decided to develop an in-house spreadsheet that could be optimised for this study based on the spreadsheet previously described by Peters et al. (2015) [54]. The modifications made are presented in Table 1. The daily results for the key parameters obtained from analysis of the NM-100 material were statistically compared with results for those same parameters from the ICP-MS software using a Student's paired t-test (n=15, p=0.05) (SM Table A4).

The in-house spreadsheet and ICP-MS software provided similar results only for ionic sensitivity and size limit detection, while a significant difference was observed for TE assessment. It is difficult to justify the difference observed for the TE calculation given the impossibility of knowing how it is calculated by the ICP-MS software, although we know that it is based on the theory presented by Pace et al. (2011) [37]. This may explain the differences between the TiO_2 diameters obtained, with diameters provided by the in-house spreadsheet being systematically greater than those obtained with the ICP-MS software. It is worth noting that the average diameter obtained with the in-house spreadsheet (158 ± 11 nm, n=15) was closer to the JRC value (162.4 ± 4.3 nm) [49] than that obtained with the ICP-MS software (130 ± 12 nm). These results reveal the benefits in developing one's own in-house spreadsheet for spICP-MS data processing. The advantages and drawbacks of these two data processing systems are described in more detail in SM Table A5. But generally speaking, although the ICP-MS software is able to process data directly and quickly, until such time as it becomes more efficient and provides open access to information on the data processing protocols used, an in-house spreadsheet is advantageous because our results were closer to the NM-100 reference value while offering additional parameters. Our in-house spreadsheet was consequently used to characterise TiO_2 NPs in the real samples analysed (see SM spreadsheet for for NPs samples).

3.3 Food sample analysis

The spICP-MS method developed in this study for TiO_2 NP characterisation was used to analyse a selection of 11 food samples (Table 2). The NPs were extracted according to the protocol described in section 2.3.2. To

analyse samples of frozen desserts and pastries, only a fraction was taken for extraction and further analysis (SM Table A1) so the results in terms of NP concentration are not reported because of the lack of representativeness of the whole sample. The dilution was optimised for each data acquisition replicate, and the number of particles detected varied between 600 and 1600, which corresponds to about 25-100 x 10^3 particles/mL with a TE of 2%. The analysis of each parameter was thus assessed based on at least 3600 particles (600 x 6 replicates).

Concerning the data comparison related to ^{48}Ti and ^{49}Ti isotopes, ^{48}Ti provided a lower sLOD, which is in agreement with Bucher et Auger (2019) [55]. Additionally, similar data were obtained in our study for both Ti isotopes (^{48}Ti and ^{49}Ti) regardless of particle diameter (see SM Fig. A5 in supplementary information). In the study of Bucher et Auger (2019) [55], the authors found significant differences between ^{47}Ti and ^{48}Ti isotopes for large particles (300-500 nm). Additionally, the size distributions obtained by using both ^{48}Ti and ^{49}Ti are similar, thus showing the lack of ^{48}Ca spectral (isobaric) interference [26,56]. This is most probably due to the marked dilution of samples required for spICP-MS measurements.

It is also worth noting that the size distributions obtained (SM Fig. A5) are non-symmetrical and look similar to a log-normal distribution as previously observed [57,58]. This non-symmetrical distribution leads to a difference between the average diameter and the median or the most frequent diameter as shown in the results (Table 2). It is therefore important that additional parameters such as median and most frequent diameters are assessed for a more comprehensive characterisation of NPs.

Concerning the analysis of food samples, TiO_2 NPs were not detected in the canned garnish, as expected, which confirms the withdrawal of E171 from the composition of this foodstuff, as claimed by the manufacturer. Regarding chewing gum, the average and most frequent diameter are consistent with those reported previously [15,17,26,59]. For the chocolate sample, the diameters obtained in this study are comparable to those obtained by de la Calle et al. (2018) [58], who also observed a difference between the mean diameter and the most frequent diameter due to a non-symmetrical size distribution. In general, the average diameter varied between 86 and 179 nm in these foodstuffs and the nanoparticular fractions between 19 and 68% (Table 2), which is consistent with data in the literature [8,12,14,25,58,60]. The lowest nanoparticular fractions (19 - 24%) were found in decorative food. In contrast, these samples had the greatest concentrations of TiO_2 NPs because the additive is one of the food's main ingredients. Coated sweets contained the lowest amount of NPs (mean of 0.12 $\times 10^9$ NPs/g). The number of NPs in the two chewing gum samples ranged from 266 to 74 billion/unit respectively. These results are comparable with those reported by Candás-Zapico et al. (2018) [59] but lower than those found by Dudefoi et al. (2018) [26]. The dissimilarities observed may arise from differences in the extraction protocols used, a

semi-quantitative protocol being used in this study as our objective was to extract a representative part of NPs present in the samples.

Finally, it is worth underlining that all the foodstuffs analysed in this study contained NPs whereas none of them were labelled as "nano" as required by EU regulations [10].

3.3. Pharmaceutical sample analysis

The spICP-MS method developed was also applied to the analysis of a selection of pharmaceuticals known to contain E171 or TiO_2 as an active compound (see SM Tables A2 and 3). Data using both ^{48}Ti and ^{49}Ti isotopes were recorded without revealing any significant differences; only the ^{48}Ti data are therefore reported for the analysis of pharmaceutical samples (Table 3). TiO_2 NPs were found in all of them. As expected, the haemorrhoid ointment contains the highest concentration of TiO_2 NPs because TiO_2 is used as an active compound and not as an additive. The sLOD was < 30 nm for the analysis of all the pharmaceutical samples, while the average diameter varied between 131 and 198 nm and the nanoparticular fractions between 13 and 45% (Table 3). The TiO_2 NPs in analgesic and antipyretic samples had a Gaussian size distribution whereas in the anti-inflammatory and the antispasmodic samples, the NPs had a log-normal size distribution (SM Fig. A6). This may explain the closeness of mean, median and most frequent diameters measured for the analgesic and antipyretic samples. The size distribution of the haemorrhoid ointment sample is similar to the analgesic and antipyretic samples, but more residual larger particles mean that although the average and median diameters are similar, they are higher than the most frequent diameter. Finally, these different size distributions can be due to a significant variation among producers [12,13] especially for the haemorrhoid ointment which do not have the E171 labelled but only "TiO_2".

4. Conclusion

This study reports the optimisation and application of a novel analytical method for characterising TiO_2 NPs in foodstuffs and pharmaceutical samples by spICP-MS. Firstly, this work focused on assessing the most accurate method to determining transport efficiency, which is one of the main experimental parameters in spICP-MS. To process the spICP-MS data, we then optimised an in-house spreadsheet to assess a panel of parameters (e.g. nanoparticular fraction and the most frequent diameter) for characterising NPs, and compared it with data provided by the ICP-MS software. This in-house spreadsheet provided a more accurate average diameter for TiO_2 NPs in the NM-100 reference material. The method was also applied to the analysis of a selection of

foodstuffs and pharmaceuticals likely to contain E171, hence demonstrating the suitability of the spICP-MS approach for the comprehensive characterisation of NPs in such samples. It can be recommended for routine application in analysis laboratories due to its cost effectiveness and sample throughput rate.

Acknowledgements

The authors would like to warmly thank Dr Katrin Löschner for agreeing to host the participating doctoral student for a week-long training course at the Technical University of Denmark, which was very useful in initiating this study. We are also grateful to Marina Amaral Saraiva for assisting in laboratory work.

Sample CRediT author statement

Lucas Givelet: Conceptualisation, Methodology, Software, Formal analysis, Investigation, Data curation, Writing - original draft, Visualisation; **Petru Jitaru:** Conceptualisation, Validation, Resources, Writing - review & editing, Supervision; **Delphine Truffier-Boutry:** Writing - review & editing, Supervision; **Laurent Noël:** Conceptualisation, Writing - review & editing, Funding acquisition; **Jean-François Damlencourt:** Writing - review & editing, Supervision, Project administration; **Thierry Guérin:** Conceptualisation, Validation, Resources, Writing - review & editing, Supervision, Project administration, Funding acquisition.

Funding

This work was jointly funded by the French Alternative Energies and Atomic Energy Commission (CEA) and the French Agency for Food, Environmental and Occupational Health & Safety (ANSES).

Compliance with Ethical Standards

Declaration of Interests

The authors declare that they have no conflicts of interest.

Ethical Approval

This article does not describe any studies with human participants or animals performed by any of the authors.

Informed consent

Informed consent was obtained from all individual participants included in the study.

List of figures

Figure 1: Comparison of calculated diameter of gold NPs with the reference diameter depending on the TE calculation method used

Figure 2: Nanoparticular fraction and mean diameter of NM-100 depending on the TE calculation method used (n=9)

Figure 3: Average diameter (a) and nanoparticular fraction (b) of a sample of E171 assessed in our work and in other studies depending on the TE calculation method used

References

[1] J. Lee, S. Mahendra, P.J.J. Alvarez, Nanomaterials in the Construction Industry: A Review of Their Applications and Environmental Health and Safety Considerations, ACS Nano. 4 (2010) 3580–3590. https://doi.org/10.1021/nn100866w.

[2] P. van Broekhuizen, F. van Broekhuizen, R. Cornelissen, L. Reijnders, Use of nanomaterials in the European construction industry and some occupational health aspects thereof, J. Nanoparticle Res. 13 (2011) 447–462. https://doi.org/10.1007/s11051-010-0195-9.

[3] A.M. Alkilany, L.B. Thompson, S.P. Boulos, P.N. Sisco, C.J. Murphy, Gold nanorods: Their potential for photothermal therapeutics and drug delivery, tempered by the complexity of their biological interactions, Adv. Drug Deliv. Rev. 64 (2012) 190–199. https://doi.org/10.1016/j.addr.2011.03.005.

[4] L. Li, Z. Gu, W. Gu, J. Liu, Z.P. Xu, Efficient drug delivery using SiO2 -layered double hydroxide nanocomposites, J. Colloid Interface Sci. 470 (2016) 47–55. https://doi.org/10.1016/j.jcis.2016.02.042.

[5] I. de la Calle, M. Menta, M. Klein, F. Séby, Screening of TiO2 and Au nanoparticles in cosmetics and determination of elemental impurities by multiple techniques (DLS, SP-ICP-MS, ICP-MS and ICP-OES), Talanta. 171 (2017) 291–306. https://doi.org/10.1016/j.talanta.2017.05.002.

[6] V. Sogne, F. Meier, T. Klein, C. Contado, Investigation of zinc oxide particles in cosmetic products by means of centrifugal and asymmetrical flow field-flow fractionation, J. Chromatogr. A. 1515 (2017) 196–208. https://doi.org/10.1016/j.chroma.2017.07.098.

[7] J. Athinarayanan, V.S. Periasamy, M.A. Alsaif, A.A. Al-Warthan, A.A. Alshatwi, Presence of nanosilica (E551) in commercial food products: TNF-mediated oxidative stress and altered cell cycle progression in human lung fibroblast cells, Cell Biol. Toxicol. 30 (2014) 89–100. https://doi.org/10.1007/s10565-014-9271-8.

[8] A. Weir, P. Westerhoff, L. Fabricius, K. Hristovski, N. von Goetz, Titanium Dioxide Nanoparticles in Food and Personal Care Products, Environ. Sci. Technol. 46 (2012) 2242–2250. https://doi.org/10.1021/es204168d.

[9] European Parliament, European Parliament and Council Directive 94/36/EC of 30 june 1994 on colours for use in foodstuffs, Off. J. Eur. Communities. L237 (1984) 13–29. https://eur-lex.europa.eu/legal-content/EN/ALL/?uri=celex:31994L0036.

[10] European Parliament, Regulation (EU) No 1169/2011 of The European Parliament and of The Council of 25 October 2011, Off. J. Eur. Union. L304 (2011) 18–63. https://eur-lex.europa.eu/legal-content/EN/ALL/?uri=CELEX%3A32011R1169 (accessed October 22, 2018).

[11] Anses, Nanomatériaux dans les produits destinés à l'alimentation, 2020. https://www.anses.fr/fr/system/files/ERCA2016SA0226Ra.pdf (accessed August 3, 2020).

[12] Y. Yang, K. Doudrick, X. Bi, K. Hristovski, P. Herckes, P. Westerhoff, R. Kaegi, Characterization of Food-Grade Titanium Dioxide: The Presence of Nanosized Particles, Environ. Sci. Technol. 48 (2014) 6391–6400. https://doi.org/10.1021/es500436x.

[13] B. Jovanović, G. Bezirci, A.S. Çağan, J. Coppens, E.E. Levi, Z. Oluz, E. Tuncel, H. Duran, M. Beklioğlu, Food web effects of titanium dioxide nanoparticles in an outdoor freshwater mesocosm experiment, Nanotoxicology. 10 (2016) 902–912. https://doi.org/10.3109/17435390.2016.1140242.

[14] J.J. Faust, K. Doudrick, Y. Yang, P. Westerhoff, D.G. Capco, Food grade titanium dioxide disrupts intestinal brush border microvilli in vitro independent of sedimentation, Cell Biol. Toxicol. 30 (2014) 169–188. https://doi.org/10.1007/s10565-014-9278-1.

[15] X.X. Chen, B. Cheng, Y.X. Yang, A. Cao, J.H. Liu, L.J. Du, Y. Liu, Y. Zhao, H. Wang, Characterization and preliminary toxicity assay of nano-titanium dioxide additive in sugar-coated chewing gum, Small. 9 (2013) 1765–1774. https://doi.org/10.1002/smll.201201506.

[16] R.J.B. Peters, G. van Bemmel, Z. Herrera-Rivera, H.P.F.G. Helsper, H.J.P. Marvin, S. Weigel, P.C. Tromp, A.G. Oomen, A.G. Rietveld, H. Bouwmeester, Characterization of Titanium Dioxide Nanoparticles in Food Products: Analytical Methods To Define Nanoparticles, J. Agric. Food Chem. 62 (2014) 6285–6293. https://doi.org/10.1021/jf5011885.

[17] J.J. Faust, K. Doudrick, Y. Yang, D.G. Capco, P. Westerhoff, A Facile Method for Separating and Enriching Nano and Submicron Particles from Titanium Dioxide Found in Food and Pharmaceutical Products, PLoS One. 11 (2016) e0164712. https://doi.org/10.1371/journal.pone.0164712.

[18] IARC Working Group on the Evaluation of Carcinogenic Risks to Humans., International Agency for Research on Cancer., Carbon black, titanium dioxide, and talc, International Agency for Research on Cancer, 2010. https://publications.iarc.fr/Book-And-Report-Series/Iarc-Monographs-On-The-Identification-Of-Carcinogenic-Hazards-To-Humans/Carbon-Black-Titanium-Dioxide-And-Talc-2010 (accessed October 15, 2019).

[19] EFSA, Re-evaluation of titanium dioxide (E 171) as a food additive, EFSA J. 14 (2016) 1–83. https://doi.org/10.2903/j.efsa.2016.4545.

[20] EFSA, Evaluation of four new studies on the potential toxicity of titanium dioxide used as a food additive (E 171), EFSA J. 16 (2018) 27. https://doi.org/10.2903/j.efsa.2018.5366.

[21] EFSA, Scientific opinion on the proposed amendment of the EU specifications for titanium dioxide (E

171) with respect to the inclusion of additional parameters related to its particle size distribution, EFSA J. 17 (2019). https://doi.org/10.2903/j.efsa.2019.5760.

[22] E. Baranowska-Wójcik, D. Szwajgier, P. Oleszczuk, A. Winiarska-Mieczan, Effects of Titanium Dioxide Nanoparticles Exposure on Human Health—a Review, Biol. Trace Elem. Res. 193 (2020) 118–129. https://doi.org/10.1007/s12011-019-01706-6.

[23] S. Bettini, E. Boutet-Robinet, C. Cartier, C. Coméra, E. Gaultier, J. Dupuy, N. Naud, S. Taché, P. Grysan, S. Reguer, N. Thieriet, M. Réfrégiers, D. Thiaudière, J.-P. Cravedi, M. Carrière, J.-N. Audinot, F.H. Pierre, L. Guzylack-Piriou, E. Houdeau, Food-grade TiO2 impairs intestinal and systemic immune homeostasis, initiates preneoplastic lesions and promotes aberrant crypt development in the rat colon, Sci. Rep. 7 (2017) 40373. https://doi.org/10.1038/srep40373.

[24] F. Peng, M.I. Setyawati, J.K. Tee, X. Ding, J. Wang, M.E. Nga, H.K. Ho, D.T. Leong, Nanoparticles promote in vivo breast cancer cell intravasation and extravasation by inducing endothelial leakiness, Nat. Nanotechnol. 14 (2019) 279–286. https://doi.org/10.1038/s41565-018-0356-z.

[25] W. Dudefoi, H. Terrisse, M. Richard-Plouet, E. Gautron, F. Popa, B. Humbert, M.-H. Ropers, Criteria to define a more relevant reference sample of titanium dioxide in the context of food: a multiscale approach, Food Addit. Contam. Part A. 34 (2017) 1–13. https://doi.org/10.1080/19440049.2017.1284346.

[26] W. Dudefoi, H. Terrisse, A.F. Popa, E. Gautron, B. Humbert, M. Ropers, Evaluation of the content of TiO2 nanoparticles in the coatings of chewing gums, Food Addit. Contam. Part A. 35 (2018) 211–221. https://doi.org/10.1080/19440049.2017.1384576.

[27] N. Kim, C. Kim, S. Jung, Y. Park, Y. Lee, J. Jo, M. Hong, S. Lee, Y. Oh, K. Jung, Determination and identification of titanium dioxide nanoparticles in confectionery foods, marketed in South Korea, using inductively coupled plasma optical emission spectrometry and transmission electron microscopy, Food Addit. Contam. Part A. 35 (2018) 1238–1246. https://doi.org/10.1080/19440049.2018.1482011.

[28] D.M. Mitrano, A. Barber, A. Bednar, P. Westerhoff, C.P. Higgins, J.F. Ranville, Silver nanoparticle characterization using single particle ICP-MS (SP-ICP-MS) and asymmetrical flow field flow fractionation ICP-MS (AF4-ICP-MS), J. Anal. At. Spectrom. 27 (2012) 1131. https://doi.org/10.1039/c2ja30021d.

[29] C. Contado, Nanomaterials in consumer products: A challenging analytical problem, Front. Chem. 3 (2015) 1–20. https://doi.org/10.3389/fchem.2015.00048.

[30] M. Mattarozzi, M. Suman, C. Cascio, D. Calestani, S. Weigel, A. Undas, R. Peters, Analytical

approaches for the characterization and quantification of nanoparticles in food and beverages, Anal. Bioanal. Chem. 409 (2017) 63–80. https://doi.org/10.1007/s00216-016-9946-5.

[31] C. Degueldre, P.-Y. Favarger, Colloid analysis by single particle inductively coupled plasma-mass spectroscopy: a feasibility study, Colloids Surfaces A Physicochem. Eng. Asp. 217 (2003) 137–142. https://doi.org/10.1016/S0927-7757(02)00568-X.

[32] C. Degueldre, P.-Y. Favarger, Thorium colloid analysis by single particle inductively coupled plasma-mass spectrometry, Talanta. 62 (2004) 1051–1054. https://doi.org/10.1016/j.talanta.2003.10.016.

[33] C. Degueldre, P.Y. Favarger, C. Bitea, Zirconia colloid analysis by single particle inductively coupled plasma-mass spectrometry, Anal. Chim. Acta. 518 (2004) 137–142. https://doi.org/10.1016/j.aca.2004.04.015.

[34] C. Degueldre, P.-Y. Favarger, S. Wold, Gold colloid analysis by inductively coupled plasma-mass spectrometry in a single particle mode, Anal. Chim. Acta. 555 (2006) 263–268. https://doi.org/10.1016/j.aca.2005.09.021.

[35] F. Laborda, J. Jiménez-Lamana, E. Bolea, J.R. Castillo, Selective identification, characterization and determination of dissolved silver(i) and silver nanoparticles based on single particle detection by inductively coupled plasma mass spectrometry, J. Anal. At. Spectrom. 26 (2011) 1362. https://doi.org/10.1039/c0ja00098a.

[36] F. Laborda, J. Jiménez-Lamana, E. Bolea, J.R. Castillo, Critical considerations for the determination of nanoparticle number concentrations, size and number size distributions by single particle ICP-MS, J. Anal. At. Spectrom. 28 (2013) 1220. https://doi.org/10.1039/c3ja50100k.

[37] H.E. Pace, N.J. Rogers, C. Jarolimek, V.A. Coleman, C.P. Higgins, J.F. Ranville, Determining Transport Efficiency for the Purpose of Counting and Sizing Nanoparticles via Single Particle Inductively Coupled Plasma Mass Spectrometry, Anal. Chem. 83 (2011) 9361–9369. https://doi.org/10.1021/ac201952t.

[38] R. Aznar, F. Barahona, O. Geiss, J. Ponti, T. José Luis, J. Barrero-Moreno, Quantification and size characterisation of silver nanoparticles in environmental aqueous samples and consumer products by single particle-ICPMS, Talanta. 175 (2017) 200–208. https://doi.org/10.1016/j.talanta.2017.07.048.

[39] J. Fuchs, M. Aghaei, T.D. Schachel, M. Sperling, A. Bogaerts, U. Karst, Impact of the Particle Diameter on Ion Cloud Formation from Gold Nanoparticles in ICPMS, Anal. Chem. 90 (2018) 10271–10278. https://doi.org/10.1021/acs.analchem.8b02007.

[40] V. Geertsen, E. Barruet, F. Gobeaux, J. Lacour, O. Taché, Contribution to Accurate Spherical Gold Nanoparticle Size Determination by Single-Particle Inductively Coupled Mass Spectrometry: A

Comparison with Small-Angle X-ray Scattering, Anal. Chem. 90 (2018) 9742–9750. https://doi.org/10.1021/acs.analchem.8b01167.

[41] B. Meermann, V. Nischwitz, ICP-MS for the analysis at the nanoscale – a tutorial review, J. Anal. At. Spectrom. 33 (2018) 1432–1468. https://doi.org/10.1039/C8JA00037A.

[42] M.D. Montaño, H.R. Badiei, S. Bazargan, J.F. Ranville, Improvements in the detection and characterization of engineered nanoparticles using spICP-MS with microsecond dwell times, Environ. Sci. Nano. 1 (2014) 338–346. https://doi.org/10.1039/C4EN00058G.

[43] I. Abad-Álvaro, E. Peña-Vázquez, E. Bolea, P. Bermejo-Barrera, J.R. Castillo, F. Laborda, Evaluation of number concentration quantification by single-particle inductively coupled plasma mass spectrometry: microsecond vs. millisecond dwell times, Anal. Bioanal. Chem. 408 (2016) 5089–5097. https://doi.org/10.1007/s00216-016-9515-y.

[44] J. Tuoriniemi, G. Cornelis, M. Hassellöv, Size Discrimination and Detection Capabilities of Single-Particle ICPMS for Environmental Analysis of Silver Nanoparticles, Anal. Chem. 84 (2012) 3965–3972. https://doi.org/10.1021/ac203005r.

[45] X. Bi, S. Lee, J.F. Ranville, P. Sattigeri, A. Spanias, P. Herckes, P. Westerhoff, Quantitative resolution of nanoparticle sizes using single particle inductively coupled plasma mass spectrometry with the K-means clustering algorithm, J. Anal. At. Spectrom. 29 (2014) 1630. https://doi.org/10.1039/C4JA00109E.

[46] L. Hendriks, A. Gundlach-Graham, D. Günther, Performance of sp-ICP-TOFMS with signal distributions fitted to a compound Poisson model, J. Anal. At. Spectrom. 34 (2019) 1900–1909. https://doi.org/10.1039/C9JA00186G.

[47] F. Laborda, A.C. Gimenez-Ingalaturre, E. Bolea, J.R. Castillo, Single particle inductively coupled plasma mass spectrometry as screening tool for detection of particles, Spectrochim. Acta Part B At. Spectrosc. 159 (2019) 105654. https://doi.org/10.1016/j.sab.2019.105654.

[48] K.A. Jensen, Y. Kembouche, E. Christiansen, J. Nicklas R, W. Hâkan, C. Guiot, O. Spalla, O. Witschger, Final protocol for producing suitable manufactured nanomaterial exposure media, 2013. https://www.anses.fr/fr/system/files/nanogenotox_deliverable.1.pdf.

[49] K. Rasmussen, J. Mast, P.-J. De Temmerman, E. Verleysen, N. Waegeneers, F. Van Steen, J.C. Pizzolon, L. De Temmerman, E. Van Doren, K.A. Jensen, R. Birkedal, M. Levin, S.H. Nielsen, I.K. Koponen, P.A. Clausen, V. Kofoed-Sørensen, Y. Kembouche, N. Thieriet, O. Spalla, C. Guiot, D. Rousset, O. Witschger, S. Bau, B. Bianchi, C. Motzkus, B. Shivachev, L. Dimowa, R. Nikolova, D.

Nihtianova, M. Tarassov, O. Petrov, S. Bakardjieva, D. Gilliland, F. Pianella, G. Ceccone, V. Spampinato, G. Cotogno, N. Gibson, C. Gaillard, A. Mech, Titanium Dioxide, NM-100, NM-101, NM-102, NM-103, NM-104, NM-105: Characterisation and Physico- Chemical Properties, 2014. https://doi.org/10.2788/79554.

[50] K.A. Huynh, E. Siska, E. Heithmar, S. Tadjiki, S.A. Pergantis, Detection and Quantification of Silver Nanoparticles at Environmentally Relevant Concentrations Using Asymmetric Flow Field–Flow Fractionation Online with Single Particle Inductively Coupled Plasma Mass Spectrometry, Anal. Chem. 88 (2016) 4909–4916. https://doi.org/10.1021/acs.analchem.6b00764.

[51] M. Loula, A. Kaňa, O. Mestek, Non-spectral interferences in single-particle ICP-MS analysis: An underestimated phenomenon, Talanta. 202 (2019) 565–571. https://doi.org/10.1016/j.talanta.2019.04.073.

[52] L. Givelet, D. Truffier-Boutry, S. Motellier, P. Jitaru, V. Bartolomei, L. Noël, T. Guérin, J.-F. Damlencourt, Characterization of TiO2 Nanoparticles in Food Additives by Asymmetric-Flow Field-Flow Fractionation Coupled to Inductively Coupled Plasma-Mass Spectrometry—a Pilot Study, Food Anal. Methods. 12 (2019) 1973–1987. https://doi.org/10.1007/s12161-019-01543-2.

[53] A.K. Venkatesan, R.B. Reed, S. Lee, X. Bi, D. Hanigan, Y. Yang, J.F. Ranville, P. Herckes, P. Westerhoff, Detection and Sizing of Ti-Containing Particles in Recreational Waters Using Single Particle ICP-MS, Bull. Environ. Contam. Toxicol. 100 (2018) 120–126. https://doi.org/10.1007/s00128-017-2216-1.

[54] R.J.B. Peters, Z. Herrera-Rivera, A. Undas, M. van der Lee, H. Marvin, H. Bouwmeester, S. Weigel, Single particle ICP-MS combined with a data evaluation tool as a routine technique for the analysis of nanoparticles in complex matrices, J. Anal. At. Spectrom. 30 (2015) 1274–1285. https://doi.org/10.1039/C4JA00357H.

[55] G. Bucher, F. Auger, Combination of 47 Ti and 48 Ti for the determination of highly polydisperse TiO 2 particle size distributions by spICP-MS, J. Anal. At. Spectrom. 34 (2019) 1380–1386. https://doi.org/10.1039/C9JA00101H.

[56] M. Lorenzetti, A. Drame, S. Šturm, S. Novak, TiO2 (Nano)Particles Extracted from Sugar-Coated Confectionery, J. Nanomater. 2017 (2017) 1–14. https://doi.org/10.1155/2017/6298307.

[57] C. Motzkus, F. Gaie-Levrel, P. Ausset, M. Maillé, N. Baccile, S. Vaslin-Reimann, J. Idrac, D. Oster, N. Fischer, T. Macé, Impact of batch variability on physicochemical properties of manufactured TiO 2 and SiO 2 nanopowders, Powder Technol. 267 (2014) 39–53. https://doi.org/10.1016/j.powtec.2014.06.055.

[58] I. de la Calle, M. Menta, M. Klein, B. Maxit, F. Séby, Towards routine analysis of TiO2 (nano-)particle size in consumer products: Evaluation of potential techniques, Spectrochim. Acta Part B At. Spectrosc. 147 (2018) 28–42. https://doi.org/10.1016/j.sab.2018.05.012.

[59] S. Candás-Zapico, D.J. Kutscher, M. Montes-Bayón, J. Bettmer, Single particle analysis of TiO2 in candy products using triple quadrupole ICP-MS, Talanta. 180 (2018) 309–315. https://doi.org/10.1016/j.talanta.2017.12.041.

[60] J.-H. Lim, D. Bae, A. Fong, Titanium Dioxide in Food Products: Quantitative Analysis Using ICP-MS and Raman Spectroscopy, J. Agric. Food Chem. 66 (2018) 13533–13540. https://doi.org/10.1021/acs.jafc.8b06571.

Figure 1

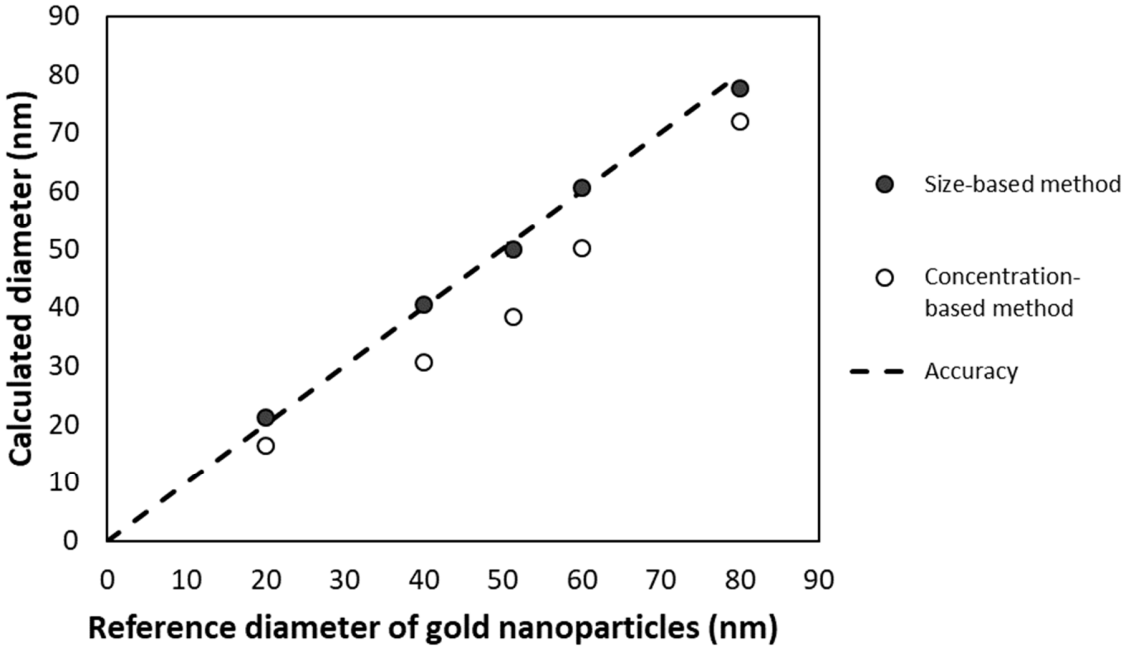
Calculated diameter (nm)
Reference diameter of gold nanoparticles (nm)
0
10
20
30
40
50
60
70
80
90
Size-based method
Concentration-based method
Accuracy

Figure 2

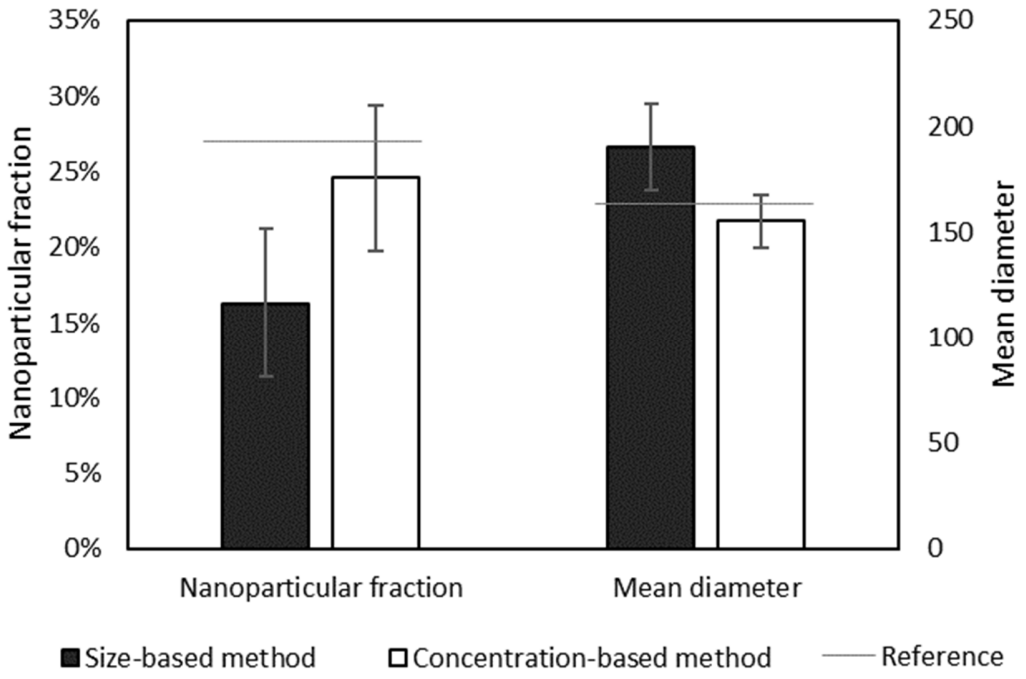
35%
30%
25%
20%
15%
10%
5%
0%
Nanoparticular fraction
250
200
150
100
50
0
Mean diameter
Nanoparticular fraction
Mean diameter
Size-based method
Concentration-based method
Reference

Figure 3

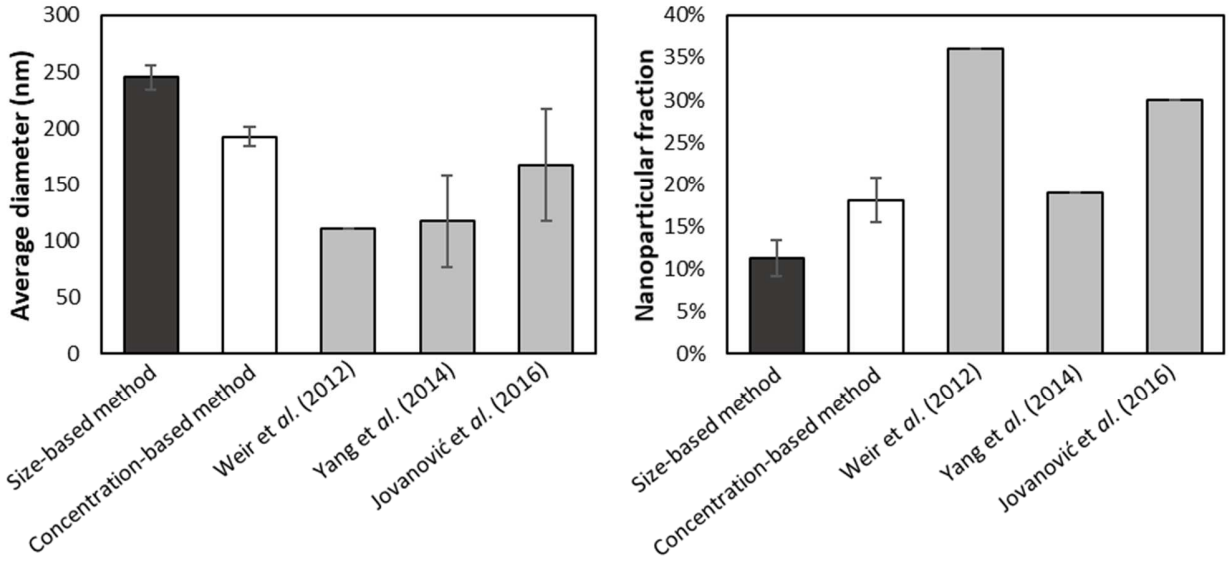
Average diameter (nm)
300
250
200
150
100
50
0
Size-based method
Concentration-based method
Weir et al. (2012)
Yang et al. (2014)
Jovanović et al. (2016)
Nanoparticular fraction
40%
35%
30%
25%
20%
15%
10%
5%
0%
Size-based method
Concentration-based method
Weir et al. (2012)
Yang et al. (2014)
Jovanović et al. (2016)

Table 1: List of the different modifications made to the Excel spreadsheet presented by Peters et al. (2015) [54]

Optimisation	RIKILT Excel spreadsheet	In-house Excel spreadsheet
Threshold calculation	Arbitrary	Automatic, the user can choose the parameters n x std
Ionic standardisation	Use the average	Use the best correlation between average and median
TE calculation	Concentration-based method	Concentration-based and size-based methods
Graph automation	Fixed gap of 2 nm, limit at 200 nm	The user can choose the gap and graphical limits adapt automatically
Size limit of detection	No	Automatic calculation from threshold
Nanoparticular fraction	No	Automatic calculation
Signal integration[a]	No	Signal integration (suitable for µs dwell time)

a: This modification was made after the dwell time optimisation experiment.

Table 2: Results obtained on real food samples by spICP-MS (n=6)

Sample	Isotope	Average diameter (nm)	Most frequent diameter (nm)	Median diameter (nm)	NP fraction (%)	NP content (x10^9 NPs/g)	LOD (nm)
Chewing gum 1	^{49}Ti	152 ± 2[a]	115 ± 3	144 ± 4	25 ± 2	44 ± 2	46 ± 1
	^{48}Ti	148 ± 3	113 ± 2	142 ± 4	27 ± 2	45 ± 4	33 ± 1
Chewing gum 2	^{49}Ti	144 ± 4	105 ± 2	129 ± 3	33 ± 3	11 ± 2	48 ± 3
	^{48}Ti	133 ± 5	99 ± 4	121 ± 5	37 ± 2	13 ± 1	29 ± 1
Chocolate	^{49}Ti	115 ± 2	92 ± 2	100 ± 4	49 ± 3	39 ± 2	48 ± 3
	^{48}Ti	100 ± 3	76 ± 2	86 ± 3	59 ± 2	49 ± 1	30 ± 1
Coated sweets	^{49}Ti	151 ± 4	113 ± 2	142 ± 3	24 ± 3	0.10 ± 0.01	55 ± 1
	^{48}Ti	137 ± 4	102 ± 3	123 ± 6	34 ± 2	0.14 ± 0.02	36 ± 1
Frozen dessert 1	^{49}Ti	131 ± 3	103 ± 2	123 ± 3	34 ± 2	NR	52 ± 1
	^{48}Ti	117 ± 3	90 ± 2	108 ± 4	46 ± 2	NR	33 ± 1
Frozen dessert 2	^{49}Ti	126 ± 4	100 ± 2	117 ± 5	37 ± 4	NR	53 ± 1
	^{48}Ti	115 ± 4	91 ± 3	108 ± 6	46 ± 4	NR	33 ± 1
Decorative food 1	^{49}Ti	195 ± 10	156 ± 16	187 ± 13	16 ± 3	52 ± 3	56 ± 1
	^{48}Ti	179 ± 7	140 ± 11	176 ± 8	24 ± 3	55 ± 3	35 ± 1
Decorative food 2	^{49}Ti	165 ± 5	123 ± 4	152 ± 4	19 ± 2	57 ± 7	49 ± 1
	^{48}Ti	163 ± 3	123 ± 3	154 ± 3	19 ± 2	57 ± 10	32 ± 1
Pastry 1	^{49}Ti	129 ± 4	101 ± 3	120 ± 6	36 ± 3	NR	46 ± 1
	^{48}Ti	125 ± 5	97 ± 3	116 ± 6	39 ± 3	NR	32 ± 2
Pastry 2	^{49}Ti	99 ± 2	87 ± 1	89 ± 4	59 ± 3	NR	47 ± 1
	^{48}Ti	86 ± 2	72 ± 4	76 ± 3	68 ± 3	NR	27 ± 0.1
Canned garnish	^{49}Ti	ND	ND	ND	ND	ND	ND
	^{48}Ti	ND	ND	ND	ND	ND	ND

NR: Not representative – ND: Not detected – a: Value ± standard deviation (SD)

Table 3: Results obtained by spICP-MS for four different pharmaceuticals (^{48}Ti monitored)

Sample	Average diameter (nm)	Most frequent diameter (nm)	Median diameter (nm)	NP fraction (%)	NP concentration (x10^9 NPs/g)	LOD (nm)
Analgesic and antipyretic	197 ± 1[a]	186 ± 4	197 ± 2	15 ± 1	16 ± 2	27 ± 1
Anti-inflammatory	140 ± 4	93 ± 4	128 ± 2	45 ± 2	113 ± 10	26 ± 1
Antispasmodic	131 ± 4	97 ± 2	125 ± 5	37 ± 2	12 ± 2	25 ± 1
Haemorrhoid ointment	198 ± 3	152 ± 3	186 ± 3	13 ± 1	201 ± 62	26 ± 2

a: Value ± SD

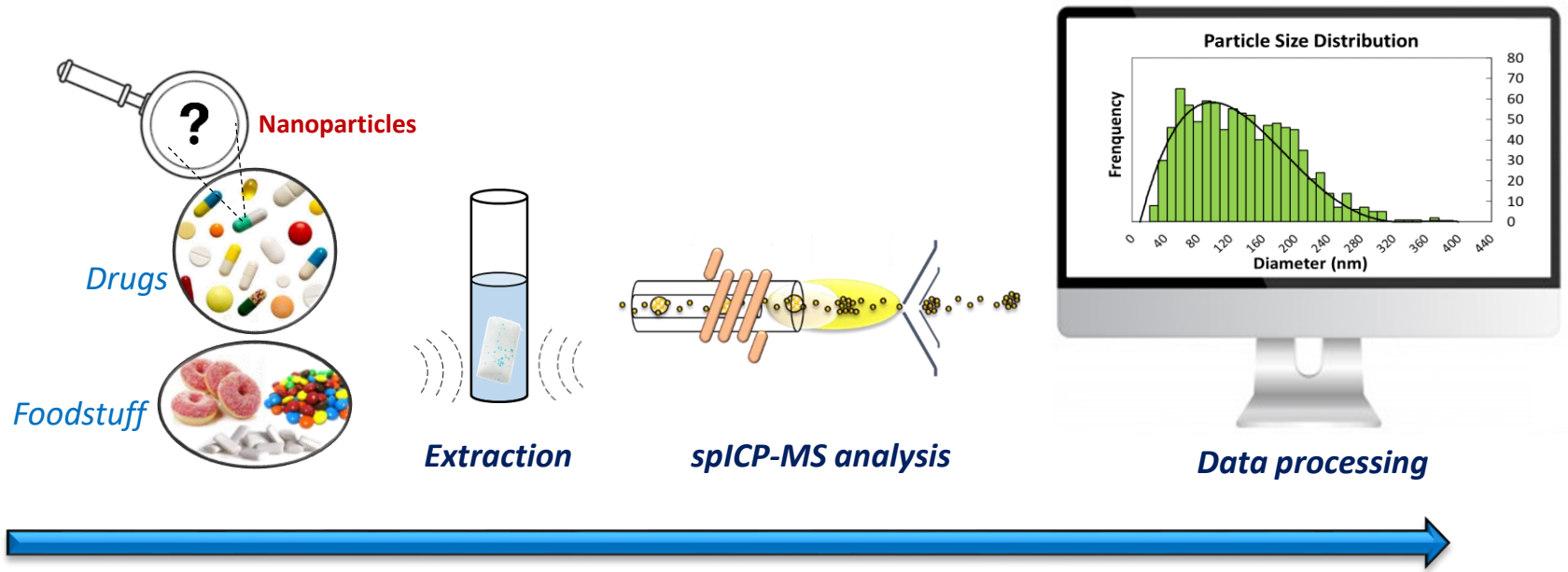
Nanoparticles
Drugs
Foodstuff
Extraction
spICP-MS analysis
Particle Size Distribution
Frenquency
Diameter (nm)
Data processing